

RESEARCH ARTICLE

Transcriptome reveals the gene expression patterns of sulforaphane metabolism in broccoli florets

Zhansheng Li^{1,2*}, Yumei Liu^{1,2}, Lingyun Li^{1,2}, Zhiyuan Fang^{1,2}, Limei Yang^{1,2}, Mu Zhuang^{1,2}, Yangyong Zhang^{1,2}, Honghao Lv^{1,2}

1 Chinese Academy of Agricultural Sciences, Institute of Vegetables and Flowers, Beijing, China, **2** The Key Laboratory of Biology and Genetic Improvement of Horticultural Crops, Ministry of Agriculture, P. R. China, Beijing, China

* lizhansheng@caas.cn



OPEN ACCESS

Citation: Li Z, Liu Y, Li L, Fang Z, Yang L, Zhuang M, et al. (2019) Transcriptome reveals the gene expression patterns of sulforaphane metabolism in broccoli florets. PLoS ONE 14(3): e0213902. <https://doi.org/10.1371/journal.pone.0213902>

Editor: Yong Pyo Lim, Chungnam National University, REPUBLIC OF KOREA

Received: April 23, 2018

Accepted: March 5, 2019

Published: March 25, 2019

Copyright: © 2019 Li et al. This is an open access article distributed under the terms of the [Creative Commons Attribution License](https://creativecommons.org/licenses/by/4.0/), which permits unrestricted use, distribution, and reproduction in any medium, provided the original author and source are credited.

Data Availability Statement: All relevant data are within the paper and its Supporting Information files.

Funding: This work was funded by the National Nature Science Foundation (31501761, 31372067) to ZL, the China Agriculture Research System (CARS-23-A8) to ZL, the National Key Research and Development Program of China (2017YFD0101805) to ZL, as well as the Science and Technology Innovation Program of the Chinese Academy of Agricultural Sciences (CAAS-ASTIP-IVFCAAS) to ZL.

Abstract

Sulforaphane is a new and effective anti-cancer component that is abundant in broccoli. In the past few years, the patterns of variability in glucosinolate content and its regulation in *A. thaliana* have been described in detail. However, the diversity of glucosinolate and sulforaphane contents in different organs during vegetative and reproductive stages has not been clearly explained. In this paper, we firstly investigated the transcriptome profiles of the developing buds and leaves at bolting stage of broccoli (B52) to further assess the gene expression patterns involved in sulforaphane synthesis. The *CYP79F1* gene, as well as nine other genes related to glucoraphanin biosynthesis, *MAM1*, *MAM3*, *St5b-2*, *FMO GS-OX1*, *MY*, *AOP2*, *AOP3*, *ESP* and *ESM1* were selected by digital gene expression analysis and were validated by quantitative real-time PCR (qRT-PCR). Meanwhile, the compositions of glucosinolates and sulforaphane were detected for correlation analysis with related genes. Finally the RNA sequencing libraries generated 147 957 344 clean reads, and 8 539 unigene assemblies were produced. In digital result, only *CYP79F1*, in the glucoraphanin pathway, was up-regulated in young buds but absent from the other organs, which was consistent with the highest level of sulforaphane content being in this organ compared to mature buds, buds one day before flowering, flowers and leaves. The sequencing results also presented that auxin and cytokinin might affect glucoraphanin accumulation. The study revealed that up-regulated expression of *CYP79F1* plays a fundamental and direct role in sulforaphane production in inflorescences. Two genes of *MAM1* and *St5b-2* could up-regulated glucoraphanin generation. Synergistic expression of *MAM1*, *MAM3*, *St5b-2*, *FMO GS-OX1*, *MY*, *ESP* and *ESM1* was found in sulforaphane metabolism. This study will be beneficial for understanding the diversity of sulforaphane in broccoli organs.

Competing interests: The authors have declared that no competing interests exist.

Introduction

In recent years, sulforaphane has attracted much interest due to its anti-cancer activity, and a growing body of epidemiological evidence has shown that increased consumption of sulforaphane or cruciferous vegetables rich in sulforaphane can lower the risk of lung [1], colon [2], pancreatic [3], breast [4], bladder [5] and prostate [6] cancers as well as some geriatric diseases such as Alzheimer's disease [7] and cardiovascular disease [8, 9]. The chemoprotective function of sulforaphane is due to its ability to induce phase II detoxification enzymes [10, 11], directly resulting in cancer cell apoptosis [12, 13].

Sulforaphane is an isothiocyanate, and it can be synthesized from glucoraphanin through hydrolysis by myrosinase when broccoli is chewed, mechanically damaged, digested by humans, or bitten by insects [14, 15]. Glucoraphanin (4-Methylsulfonylbutyl glucosinolate) is a glucosinolate mostly found in *Brassica* vegetables, such as broccoli, cabbage (green and red), Chinese kale, Brussels sprouts, kohlrabi, collards, and turnip [16–18]. Among the crucifers tested, broccoli has been reported to be rich in glucoraphanin, and the regulation of glucosinolate synthesis has been largely reported in *A. thaliana* [19–22].

Glucosinolates are mainly synthesized from amino acids Met, Phe and Trp, which accordingly give rise to three groups of glucosinolates: aliphatic glucosinolates, benzenic glucosinolates and indolic glucosinolates [15, 22–24]. Regulation genes of glucosinolate and the pathway have been successfully identified in *Arabidopsis* [23, 25–27]. Glucoraphanin belongs to aliphatic glucosinolate derived from Met. In the process of chain elongation, it starts with deamination by a BCAT4 giving rise to a 2-oxo-4-methylthiobutanoic acid. The 2-oxo-4-methylthiobutanoic acid then enters a cycle of three successive transformations: condensation with acetyl-CoA by *MAM1* and *MAM3*, isomerization by *IPMI-SSU2*, 3, and oxidative decarboxylation by *IPM-DH*, generating 2-Oxo-6-methylthiohexanoic acid [16, 28].

A total of 13 enzymes, representing five different biochemical steps in the formation of the glucosinolate core structure, have been characterized [24, 29]. For the core biosynthetic pathway of aliphatic glucosinolates, *CYP79F1* (Met1-6), *CYP79F2* (Met 5, 6), *CYP83A1*, *GSTF11*, *GSTU20*, *GGP1*, *SUR1* (*C-S lyase*), *UGT74C1*, *SOT17* (*AtSTb*), and *SOT18* (*AtSTb*) play distinct roles in oxidation, conjugation, C-S cleavage, glucosylation and sulfation functions, then 2-oxo-6-methylthiohexanoic acid and dihomomethionine are transferred to 4-methylthiobutyl glucosinolate (glucoerucin). Finally, glucoerucin is oxidized and changed into glucoraphanin by *FMO-GSOX1-5* [26, 30].

The following process is secondary modification, and the biological activity of glucosinolates is determined by the structure of the side chain [22, 27]. In aliphatic glucosinolates, 4-methylthiobutyl actually is the precursor of glucoraphanin, is catalyzed to generate 3-pentenyl glucosinolate (gluconapin) by *GS-ALK*, as well as 4-benzoyloxybutyl glucosinolate by *GS-OHB*. Glucoraphanin can also be hydrolyzed to sulforaphane catalyzed by myrosinase (*MY*) or, depending on pH, more sulforaphane is generated in an alkaline environment [28, 31, 32]. Together with side-chain elongation, secondary modifications are responsible for more than 132 known glucosinolate structures [33, 34], of which there have been 56 putative genes identified in glucosinolate pathway of *B. oleracea* (http://www.ocri-genomics.org/cgi-bin/bolbase/pathway_detail.cgi?entry=map00966) [35], and 110 in *B. rapa* (<http://brassicadb.org/brad/glucoGene.php>) [36, 37].

By 2010, approximately 29 genes have been found in aliphatic glucosinolate pathway [26, 38–40]. Glucosinolate synthesis and its regulation mechanism has been revealed mostly in *Arabidopsis*. However, glucosinolates are affected by many factors, such as genotypes, organs, development stages, cultivation conditions, soil microbes, and environments [22, 27, 31]. Some research and our previous work have reported that the significant differences of sulforaphane and glucoraphanin happened in different organs of *Brassica* vegetables [16, 28, 41].

But there are few reports that can explain the diversity of sulforaphane contents in different broccoli organs at various developmental stages [42, 43]. And one of the best methods to elucidate these mechanisms is to study them at the molecular level by transcriptome analysis.

In our study, it was found that the contents of glucoraphanin and sulforaphane were both in a high level with significant differences in developing buds. So the buds at bolting stage were chosen and carried out by transcriptome analysis for exploring the gene expression patterns of sulforaphane. The aims of our research were to (i) identify and validate differential expression of specific genes in developing buds (LN_B1-B4) and leaves (LN_F) individually, and (ii) find genes related to sulforaphane metabolism. Our results would provide new insights into explanation of sulforaphane accumulation in different organs of broccoli.

Materials and methods

Plant material

Broccoli inbred line B52 was cultured and treated using the method described in our previous research, and this inbred line was bred at the Institute of Vegetables and Flowers, Chinese Academy of Agricultural Sciences (CAAS-IVF) [41]. All plants were planted in greenhouse on August 2, 2015, florets formed on October 15 and bolting on November 22. At the same time, the developmental buds and leaves (LN_F) were collected at bolting stage, and the organs were young buds (LN_B1), mature buds (LN_B2), buds one day before flowering (LN_B3) and flowers (LN_B4) (Fig 1).

Library construction, sequencing and bioinformatics analysis

Total RNA was extracted from each sample by using TRIzol reagent (Invitrogen, CA, USA), and its quality was monitored on 1% agarose gels and assessed by a Bioanalyzer 2100 system (Agilent Technologies, Santa Clara, CA, USA) with a minimum RNA integrity number (RIN) of 7.0. Sequencing libraries were generated using the NEBNext Ultra RNA Library Prep Kit for Illumina (NEB, USA), and index codes were assigned to each sample. Library quality was assessed on the Agilent Bioanalyzer 2100 system. Clustering of the index-coded samples was performed on a cBot Cluster Generation System using the TruSeq PE Cluster Kit v3-cBot-HS (Illumina). After cluster generation, the prepared libraries were sequenced on an Illumina HiSeq 2500/4000 platform (Illumina, Inc., San Diego, CA, USA), which was conducted by Beijing Allwegene Technology Co., Ltd, China. Before assembly, raw reads of the cDNA libraries were filtered to remove adaptor sequences, low-quality reads containing poly-N and sequences with more than 5% unknown nucleotides. After transcriptome assembly, each unigene was annotated using five databases [44, 45]: NCBI non-redundant protein (Nr), Eukaryotic Ortholog Groups (KOG), Protein family (Pfam), Swiss-Prot, and Kyoto Encyclopedia of Genes and Genomes (KEGG) databases. Blast all software was used to predict and classify the KOG and KEGG pathway-associated unigenes [46, 47], employing BlastX (v.2.2.28C) with an E-value of less than $1e^{-5}$. Gene Ontology (GO) annotations were analyzed using Goseq [48].

Analysis of differentially expressed genes

All sequencing reads for five samples were remapped to the reference sequences using RSEM software, and the abundance of each assembled transcript was evaluated using FPKM [49–50]. For genes with more than one alternative transcript, the longest transcript was selected to calculate the FPKM. The DESeq package (ver.2.1.0) was employed to detect DEGs between sample pairs (LN_B1 versus LN_F, LN_B2 versus LN_F, LN_B3 versus LN_F and LN_B4 versus LN_F [51, 52]. The false discovery rate (FDR) was applied to correct the *p*-value threshold in

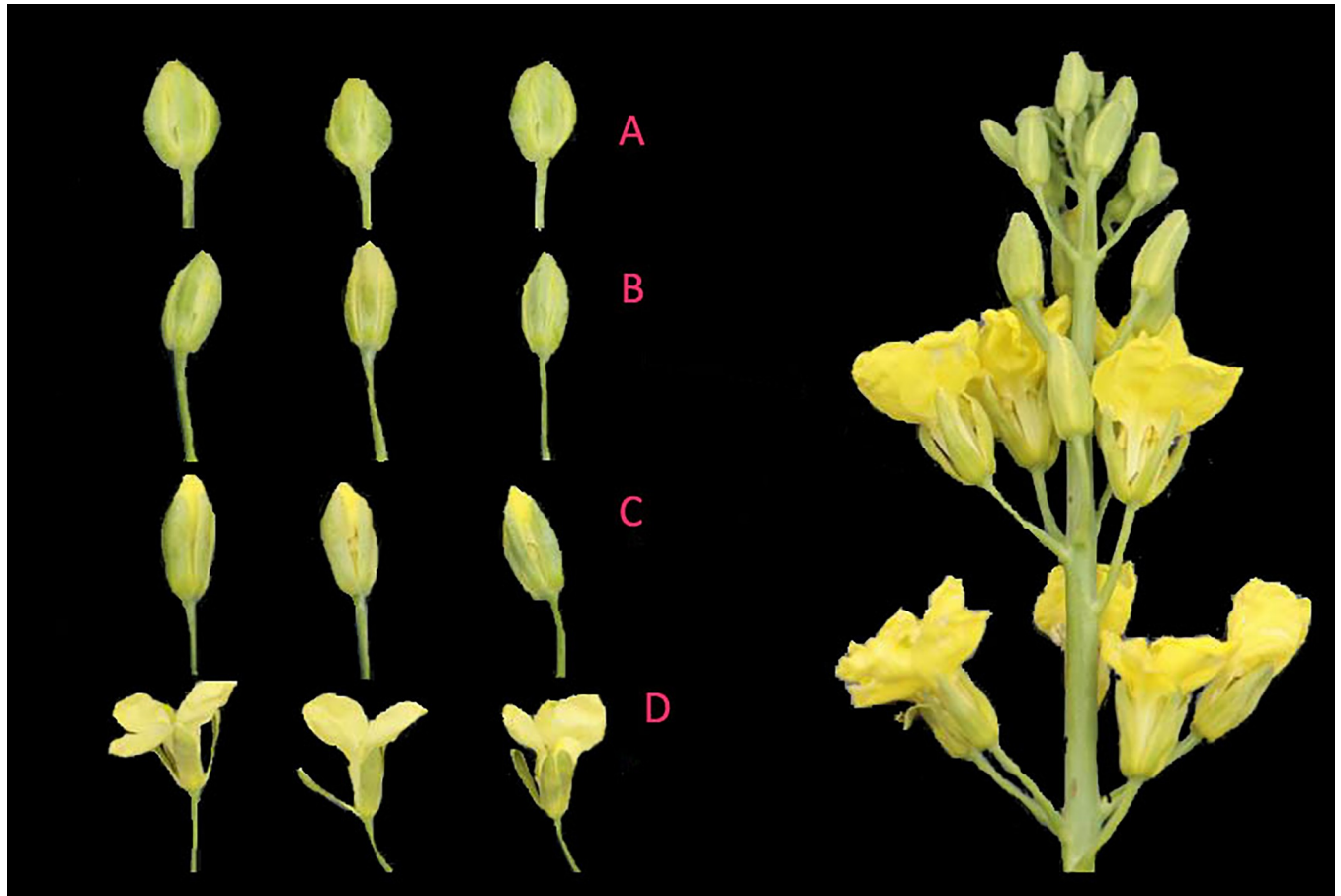


Fig 1. The developmental buds of young buds (A), mature buds (B), buds one day before flowering (C) and flowers (D) at bolting stage.

<https://doi.org/10.1371/journal.pone.0213902.g001>

multiple tests [52]. An FDR-adjusted p -value (q -value) ≤ 0.05 and a $|\log_2 \text{Fold Change}| > 1$ were used as the thresholds for identifying significant differences in gene expression. For convenience, DEGs with higher expression levels in buds compared to leaves were designated up-regulated, whereas those with lower expression were designated down-regulated [50].

Candidate glucosinolate genes selection and certification of relative expression

To verify the reliability of the expression analysis, ten candidate glucosinolate genes of *MAM1*, *MAM3*, *CYP79F1*, *St5b-2*, *FMO GS-OX1*, *MY (TGG1)*, *AOP2* and *AOP3*, *ESP* and *ESM1* were selected and quantified by real-time PCR. The primers for these genes were listed in Table 1. Samples of developing buds and leaves were gathered, and qRT-PCR analysis was performed by the method described in our previous study [41], qRT-PCR was carried out using SYBR Premix Ex TaqII (Tli RNaseH Plus; TAKARA BIO, Inc., Shiga, Japan) on an ABI 7900HT (Applied Biosystems, Carlsbad, CA, USA).

Investigation of glucosinolate genes associated with sulforaphane

To gain overall insight into differential gene expression patterns between developing buds and leaves. Ten regulated genes related to the sulforaphane pathway were chosen for confirmation

Table 1. The qRT-PCR genes related sulfuraphane metabolism and their primers.

No	Gene names	Primer sequences
1	<i>MAM1</i> Forward primer	GAGTAGACATCATGGAAGTCGGTT
	<i>MAM1</i> Reverse primer	AAGTCGCCTCAATGTCTCTATGTT
2	<i>MAM3</i> Forward primer	CGAAGTGACGATCAACGGAA
	<i>MAM3</i> Reverse primer	GACATTTCAAAGCCATCACGAC
3	<i>CYP79F1</i> Forward primer	GTCACGCCAGACGAAATCAAA
	<i>CYP79F1</i> Reverse primer	GCACAAGCCTGTCTTTTCCAAC
4	<i>FMO GS-OX1</i> Forward primer	GGAAAGCAGATCCATAGCCACA
	<i>FMO GS-OX1</i> Reverse primer	CATAGATTGTTTTGGGCACTG
5	<i>AOP2</i> Forward primer	AGTAAGAGTGACCGAGAAAAGAGG
	<i>AOP2</i> Reverse primer	GCGACCAGCTTCTGAGTGATAG
6	<i>AOP3</i> Forward primer (homologous domain)	AGGTGAAGACCAAGAGGGGAA
	<i>AOP3</i> Reverse primer (homologous domain)	TCGGTGATACGGTGAAGGGA
7	<i>MY</i> Forward primer	GCTGTGAGGTGTGAGCGGTAA
	<i>MY</i> Reverse primer	GTCTCATAAGTTAGAATTGACGCCA
8	<i>St5b-2</i> Forward primer	CCCATATACCCAACGGGTGCG
	<i>St5b-2</i> Reverse primer	CCCATGAACTCAGCCAACCT
9	<i>ESP</i> Forward primer	GATCAAGGTGGGGCAGAAAG
	<i>ESP</i> Reverse primer	AAGGTTTCGCTCCTGTAGTCTCTA
10	<i>ESM1</i> Forward primer	AAGATCTTCCACAAACCTATTG
	<i>ESM1</i> Reverse primer	TTTGTATTCTTGTCTCACGATC
11	actin-12 Forward primer	GGCTCTATCTTGGCTTCTCTCAGT
	actin-12 Reverse primer	CCAGATTCATCATACTCGGCTTT

<https://doi.org/10.1371/journal.pone.0213902.t001>

by quantitative real-time PCR (qRT-PCR). These genes are *MAM1*, *MAM3*, *CYP79F1*, *St5b-2*, *FMO GS-OX1*, *AOP2*, *AOP3*, *MY*, *ESP* and *ESM1*.

Extraction and determination of sulfuraphane and glucoraphanin

Five samples were pretreated and dried in a lyophilizer, HPLC and UHPLC–Triple–TOF–MS methods were used for determination of sulfuraphane and glucoraphanin separately. The extraction and determination methods of sulfuraphane are thoroughly described in our previous study [41, 53].

The methods for analysis of glucoraphanin and the other glucosinolates was carried out by using UHPLC–Triple–TOF–MS. Samples were extracted using 70% methanol and injected after concentration of the standard glucoraphanin. UPLC BEH C₁₈ (2.1 mm × 100 mm, 1.7 μm) column was selected with acetonitrile–water (both 0.1% formic acid) as mobile phase. Chromatographic separation was achieved under gradient elution in 10 min. In ESI negative ion mode, TOF–MS scan–IDA–Product ion scan was performed to acquire both MS and MS/MS information from one injection. Based on high resolution TOF–MS, accurate masses of molecular ions and fragment ions were obtained for high accuracy–identification.

Results

Sequencing, assembly and functional annotation

A pooled cDNA library of five samples of developing buds and leaves was analyzed on the Illumina HiSeq 2500/4000 platform (Illumina, Inc., San Diego, CA, USA). The library generated 147.96 million raw reads (Tables 2 and 3), and the assembled raw reads (>95.23%) had Phred-

like quality scores at the Q20 level (an error probability of 0.01–0.02%). Finally 48 852 unigenes of 150 bp generated based on PE150. The Gene Ontology (GO) database assigned 27 606 unigenes into 30 functional categories. The largest proportion was represented by biological process (GO 0008150, 11.86%) and metabolic process (GO 0008152, 12.39%; [S1 Fig](#)). In total, 6656 unigenes were categorized into 4 Clusters of Orthologous Groups of Proteins (COG) classifications ([S2 Fig](#)), which was shown and validated by Venn diagram comparisons ([Fig 2A](#)) and cluster analysis of differentially expressed genes between leaves and developmental buds ([Fig 2B](#)). The 3450 assembled sequences were mapped to the reference canonical pathway in the Kyoto Encyclopedia of Genes and Genomes (KEGG). In the top 20 KEGG pathways, the pathway most strongly represented by the mapped unigenes was biological process and metabolism (KO 03010, 263 unigenes) ([Fig 3](#)).

Identification and annotation of differentially expressed genes

Approximately 29.88–51.52 million 150 bp paired-end reads were generated through RNA sequencing ([S3 Fig](#)). Transcript levels were calculated using fragments per kilobase per million reads (FPKM; [Table 3](#)). The GC content from the 10 libraries ranged from 45.09 to 46.23%, and the Q30 values (reads with an average quality scores > 30) were all in the range of 89.81 to 97.90%, indicating that the quality and accuracy of sequencing data were sufficient for further analysis ([Table 2](#)). The percentage of sequenced reads from all libraries that remapped to the assembled reference transcripts was nearly $\geq 70\%$ ([Table 1](#)). According to the cabbage reference genome, 8539 genes of 45758 unigenes were functionally annotated with an e-value $\geq 1e^{-5}$ in at least one database.

Differential expression in young buds (LN_B1), mature buds (LN_B2), buds one day before flowering (LN_B3), flowers (LN_B4) and leaves (LN_F) of broccoli at bolting stage (FPKM > 5.0 in at least one treatment group, fold change ≥ 2.0 , $P \leq 0.05$) was found for 4775 to 5956 genes. Of these, 2534 to 3101 were up-regulated and 2000 to 2974 were up-regulated in all four groups of developing buds versus leaves ([Table 4](#)). The detailed gene numbers at different interval are shown in [Table 5](#), and most genes were within an FPKM Interval 0~1 (49.85%–58.35%), particularly in leaves, followed by the buds one day before flowering, flowers and mature buds ([Table 4](#)). As shown in [Fig 4A](#), we found that low expression genes were enriched in leaves, followed by buds one day before flowering, flowers, mature buds and young buds. However, young buds had higher overall gene expression, the second was mature buds, flowers, buds one day before flowering, and leaves showed the least ([Fig 2A](#)). Pearson correlations between five organs were calculated to investigate relationship of developing buds and leaves ([Fig 4B](#)). There was a gradual decrease in developing buds from young buds to flowers (LN_B1~4), which was consistent with the phenotype. In contrast, leaves displayed a varying relationship, which were most similar to young buds. All the differentially expressed genes were annotated by the databases described above.

Investigation of the glucosinolate genes associated with sulforaphane metabolism

The expression of the glucosinolate genes, including glucosinolate core genes and secondary metabolic genes were confirmed by qRT-PCR. Most of these genes showed similar trends in RNA sequencing and qRT-PCR ([Fig 5](#)). In this study, ten genes were investigated and compared with sulforaphane concentrations measured by HPLC. It was found that unlike *CYP79F1* and *AOP3*, the genes *MAM1*, *MAM3*, *St5b-2*, *FMO GS-OX1*, *MY*, *AOP2*, *ESP* and *ESM1* displayed a low expression level compared to the leaf control. There was a significantly higher expression of *CYP79F1* in the young buds compared to the other organs at this stage, following by flowers and mature buds and buds one day before flowering, and leaves had at

Table 2. Comparison of reads and reference sequence.

Sample	LN_F	LN_B1	LN_B2	LN_B3	LN_B4
Total reads	70435770	79567320	51953284	45781558	48176756
Total mapped	50627502 (71.88%)	57043101 (71.69%)	37400419 (71.99%)	33219629 (72.56%)	33514062 (69.56%)
Multiple mapped	1760525 (2.5%)	1385966 (1.74%)	1048692 (2.02%)	894641 (1.95%)	740476 (1.54%)
Uniquely mapped	48866977 (69.38%)	55657135 (69.95%)	36351727 (69.97%)	32324988 (70.61%)	32773586 (68.03%)
Read-1	25396488 (36.06%)	28907373 (36.33%)	18828753 (36.24%)	16742405 (36.57%)	17539166 (36.41%)
Read-2	23470489 (33.32%)	26749762 (33.62%)	17522974 (33.73%)	15582583 (34.04%)	15234420 (31.62%)
Reads map to '+'	24496371 (34.78%)	27873454 (35.03%)	18184082 (35%)	16172019 (35.32%)	16390884 (34.02%)
Reads map to '-'	24370606 (34.6%)	27783681 (34.92%)	18167645 (34.97%)	16152969 (35.28%)	16382702 (34.01%)
Non-splice reads	32180436 (45.69%)	34794098 (43.73%)	23101224 (44.47%)	21927513 (47.9%)	21693113 (45.03%)
Splice reads	16686541 (23.69%)	20863037 (26.22%)	13250503 (25.5%)	10397475 (22.71%)	11080473 (23%)

<https://doi.org/10.1371/journal.pone.0213902.t002>

the lowest expression level (Fig 5). AOP3 also showed a high gene expression similarly to CYP79F1, but the highest-expressing organ was flowers, and second were young buds followed by mature buds and buds one day before flowering, with leaves having the lowest level.

The same changing trends of sulforaphane and glucoraphanin happened to B52 at bolting stage, and there was an obvious decrease in sulforaphane and glucoraphanin concentrations from young buds to leaves (Fig 6A). Also there was a sharp decrease to mature buds from young buds, then another decrease from flowers to leaves. The corresponding sulforaphane contents were 3370.44, 2140.34, 1323.98, 1090.46, 235.82 mg/kg DW, respectively (Fig 6A and 6C). The corresponding contents of glucoraphanin were 43.83, 21.82, 24.65, 11.14 and 2.27 μM/g DW (Fig 6A and 6D). So the generation efficiency of sulforaphane from glucoraphanin was 30.3% to 58.6% in these organs. Except the buds one day before flowering, the other organs showed the similar efficiency, suggesting there should be no difference of myrosinase activity (ESM1) in catalyzing glucoraphanin into sulforaphane. At the same time, another 11 glucosinolates were detected in our study (Fig 6B), and gluconapin, gluotropaeolin, progoitrin and sinigrin were not determination. The result provided a good evidence for previous reports. This result showed the pattern of sulforaphane accumulation in different organs was consistent with our previous reports [41, 53].

Discussion

The glucosinolate pathway and sulforaphane metabolism

In the past 30 years, 16 natural glucosinolates in broccoli and 26 glucosinolates in *A. thaliana* have been elucidated. The total number of documented glucosinolates from plants has been 122 types [54–56].

Table 3. Sequencing and assembly statistics for the 10 transcriptomes of the B52 inbred line at bolting stage.

Sample	Raw Reads	Raw Bases	Clean Reads	Clean Bases	Error Rate	Q20	Q30	GC Content
LN_F_1	36374237	5.45Gb	35217885	5.28Gb	0.01%	99.26%	97.90%	46.15%
LN_F_2	36374237	5.45Gb	35217885	5.28Gb	0.01%	97.27%	94.13%	46.23%
LN_B1_1	41132570	6.16Gb	39783660	5.97Gb	0.01%	99.27%	97.94%	45.84%
LN_B1_2	41132570	6.16Gb	39783660	5.97Gb	0.01%	97.31%	94.23%	45.90%
LN_B2_1	26796422	4.01Gb	25976642	3.9Gb	0.01%	99.26%	97.90%	45.70%
LN_B2_2	26796422	4.01Gb	25976642	3.9Gb	0.01%	97.46%	94.51%	45.75%
LN_B3_1	23634550	3.54Gb	22890779	3.43Gb	0.01%	99.22%	97.81%	45.09%
LN_B3_2	23634550	3.54Gb	22890779	3.43Gb	0.01%	97.45%	94.49%	45.17%
LN_B4_1	25283977	3.79Gb	24088378	3.61Gb	0.01%	98.75%	96.66%	45.49%
LN_B4_2	25283977	3.79Gb	24088378	3.61Gb	0.02%	95.23%	89.81%	45.75%

<https://doi.org/10.1371/journal.pone.0213902.t003>

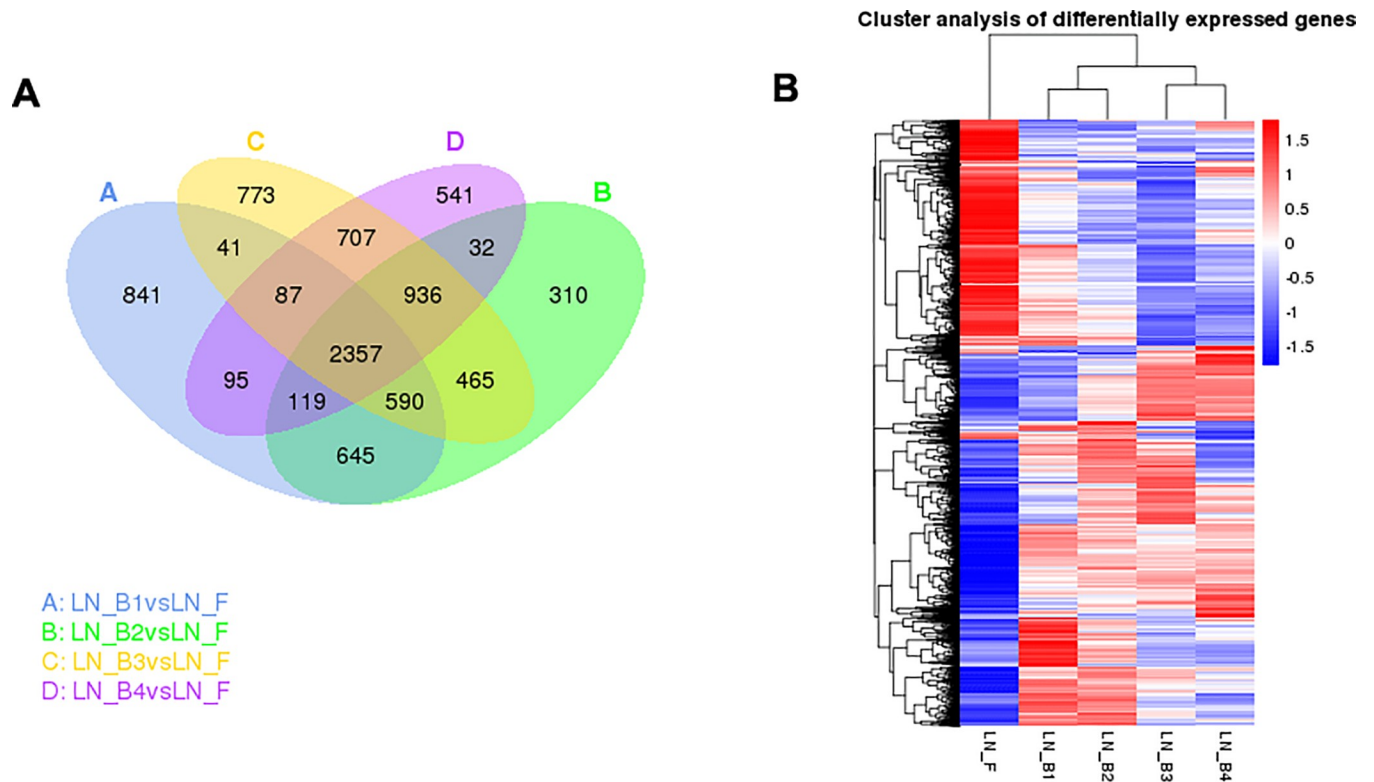


Fig 2. Venn diagram comparisons (A) and cluster analysis of differentially expressed genes between leaves and developmental buds (B). Venn diagram comparison of differentially expressed genes between leaves and developmental buds at bolting stage. Hierarchical cluster analysis of differentially expressed genes among genotypes. The color key represents Lg (RPKM + 1). Red indicates high relative expression and blue indicates low relative expression. LN_F denotes leaves and LN_B (1–4) denotes developmental buds of broccoli at bolting stage.

<https://doi.org/10.1371/journal.pone.0213902.g002>

The aliphatic pathway, encompassing 29 genes in *Arabidopsis*, was reviewed in 2010 [23, 31, 57]. Homologs for most of these genes can be found in broccoli, but different copies and variations are usually found in *Brassica* plants, such as AOP family genes [58, 59], which are responsible for the conversion of glucoraphanin to gluconapin in *Arabidopsis*. There are 3 AOP copies in broccoli, of which one is functional and two are mutated, whereas three genes in *B. napa* are functional [35]. According to sequence alignments acids, the AOP1 gene has an extra intron in exon 2, produces a smaller predicted protein and may not be functional [58, 60]. The AOP2 gene has few base changes and no function, and there is a large deletion in exon 2 in AOP3, but this gene might still retain its function. AOP3 was not found in *B. napa* [58, 60, 61]. Another gene, FMO GS-OX1, is responsible for the conversion of glucoerucin into glucoraphanin, which is important for sulforaphane generation. However, there are few differences between broccoli plants [39]. In *Arabidopsis*, the MAM family contains three tandemly duplicated and functionally diverse members (MAM1, 2, 3). MAM1 and MAM2 catalyze the condensation of the first two elongation cycles for the synthesis of the dominant C3 and C4 side chain aliphatic glucosinolates, respectively [62, 63], whereas MAM3 is assumed to contribute to the production of all glucosinolate chain lengths [22]. However, in *B. rapa* and *B. oleracea*, MAM1/MAM2 genes experienced independent tandem duplication to produce C6 and C5 orthologs, respectively [24, 35]. In addition to the MAM3 homologs in *Brassica*, at least two MAM3 genes seem to be involved the C-side chain size: BoGSL-PRO and BoGSL-ELONG, determining glucosinolate of C3 and C4 side chains, respectively [60, 64].

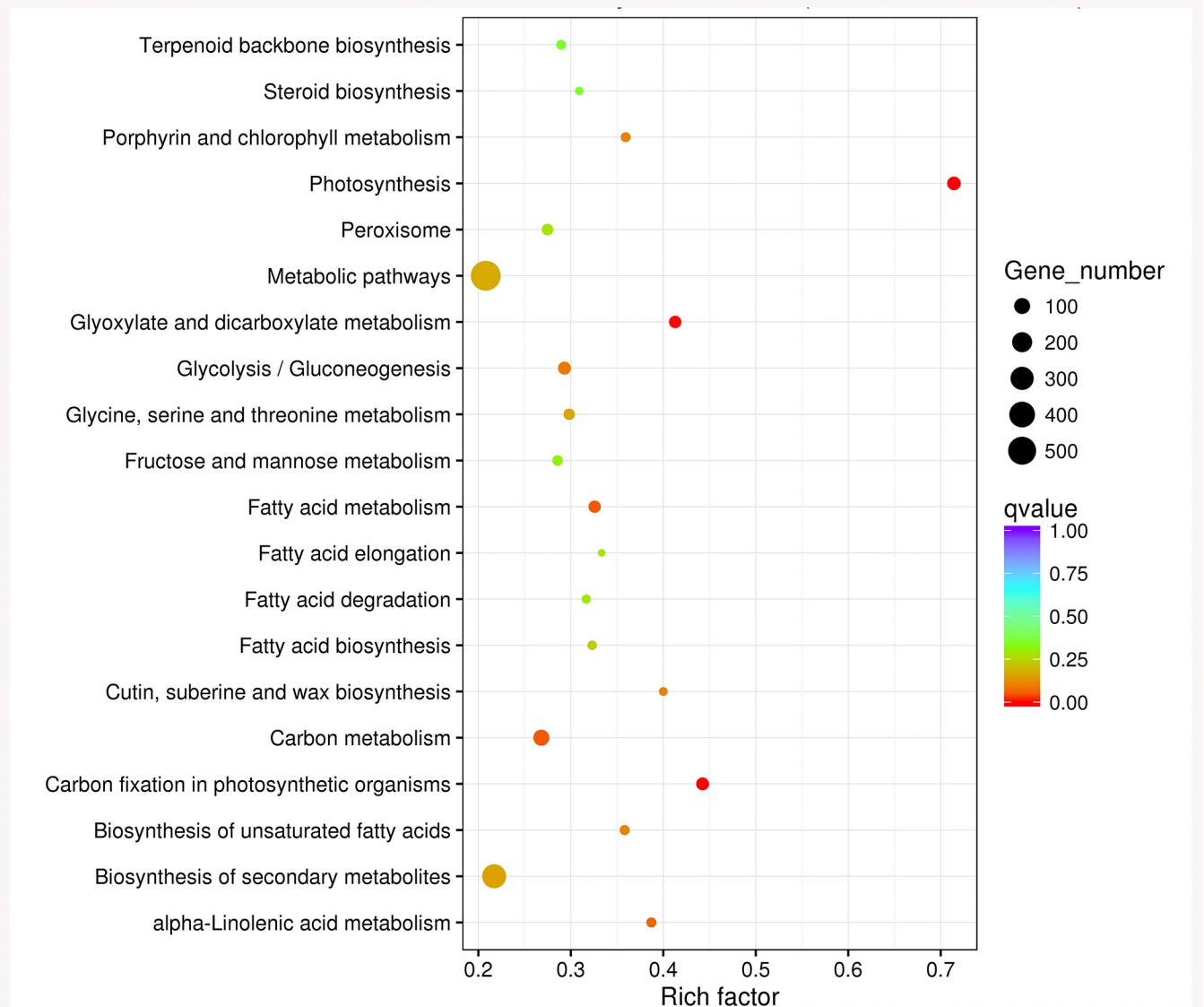


Fig 3. The top 20 KEGG pathways with the highest representation of common DEGs from pairwise comparisons between developmental buds and leaves.

<https://doi.org/10.1371/journal.pone.0213902.g003>

In this study, the genes of *MAM1*, *MAM3*, *CYP79F1*, *St5b-2*, *FMO GS-OX1*, *MY*, *AOP2*, *AOP3* (homologous domain), *ESP* and *ESM1* were detected and analyzed by qRT-PCR.

Table 4. The number of differentially expressed genes between different pairs samples.

Groups/samples	Total number	Up-regulated	Down-regulated
LN_B1 vs LN_F	4775	2775	2000
LN_B2 vs LN_F	5454	3101	2353
LN_B3 vs LN_F	5956	2982	2974
LN_B4 vs LN_F	4874	2534	2340

<https://doi.org/10.1371/journal.pone.0213902.t004>

Table 5. The statistics of gene numbers at different interval level.

FPKM Interval	LN_F	LN_B1	LN_B2	LN_B3	LN_B4
0~1	35975(58.35%)	30733(49.85%)	32042(51.97%)	33284(53.99%)	33231(53.90%)
1~3	4779(7.75%)	5840(9.47%)	5558(9.02%)	5628(9.13%)	5349(8.68%)
3~15	10372(16.82%)	12451(20.20%)	12218(19.82%)	12405(20.12%)	12054(19.55%)
15~60	7365(11.95%)	9008(14.61%)	8396(13.62%)	7332(11.89%)	7832(12.70%)
>60	3159(5.12%)	3618(5.87%)	3436(5.57%)	3001(4.87%)	3184(5.16%)

<https://doi.org/10.1371/journal.pone.0213902.t005>

Combined with the transcriptome data, the study would help us to reveal the gene expression patterns of sulforaphane in the developmental buds at bolting stage.

Glucoraphanin belongs to C4 glucosinolate, which might be produced by *MAM1/MAM2* genes. In *B. rapa*, *MAM3* plays an important role in accumulation of C5 glucosinolates, such as glucobrassicinapin [35, 37]. However, our results showed that leaves had a higher level of *MAM1* gene expression than the developing buds, which was depending on the cultivar of broccoli (Fig 5), and all the materials in this study had a low level of *MAM1* as well as *MAM3* expression, with the exception of the flowers, which had a slightly higher expression. This was consistent with the transcriptome results, which showed no significant differences between *MAM1* and *MAM3*. In this study, the sulforaphane and glucoraphanin contents in developing buds were inversely correlated with the developmental stages, which might be caused by low *MAM1* gene expression after bolting [31, 65].

A. thaliana with the *CYP79F2* gene knocked out showed substantially reduced long-chain aliphatic glucosinolates and increased short-chain aliphatic glucosinolates, and *CYP79F1*

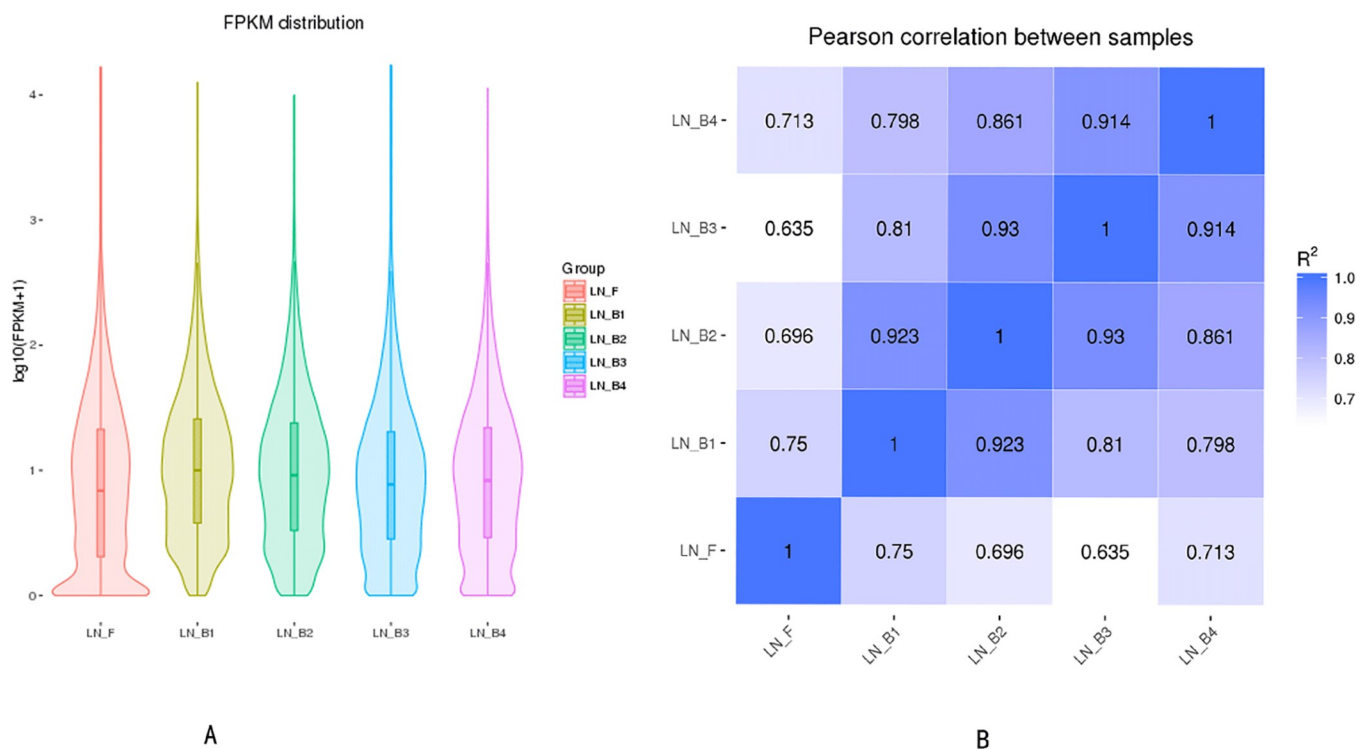


Fig 4. Violin plot of the normalized FPKM values for gene expression in different groups (A). Absolute magnitude (log) of the divergence of absolute magnitude of log (FPKM+1) resulting from leaves (LN_F), young buds (LN_B1), mature buds (LN_B2), buds one day before flowering (LN_B3) and flowers (LN_B4) of broccoli at bolting stage. **Pearson correlation between samples of developmental buds (LN_B1~4) and leaves (LN_F) (B).**

<https://doi.org/10.1371/journal.pone.0213902.g004>

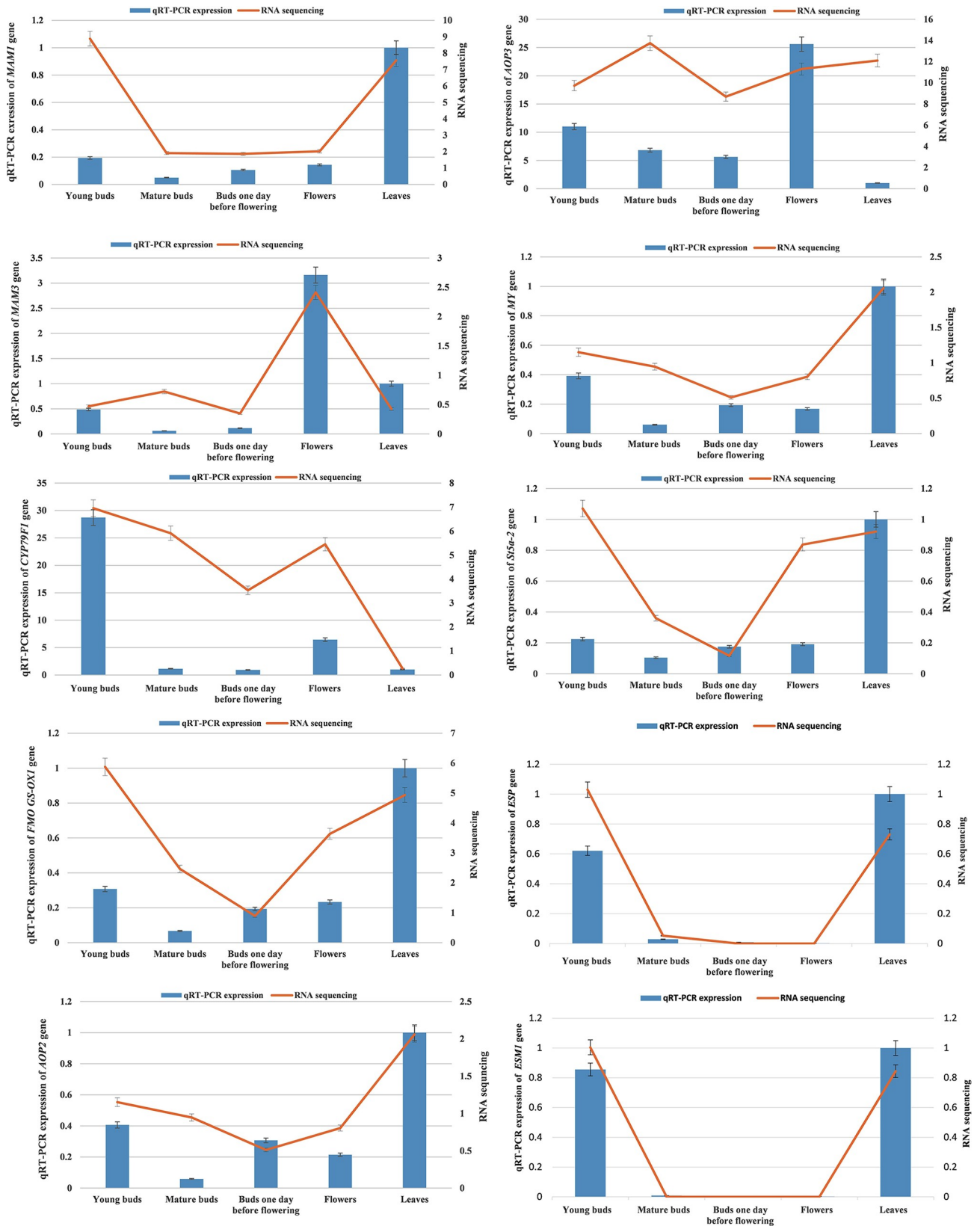


Fig 5. RNA sequencing and qRT-PCR results of the expression genes related with sulforaphane metabolism.

<https://doi.org/10.1371/journal.pone.0213902.g005>

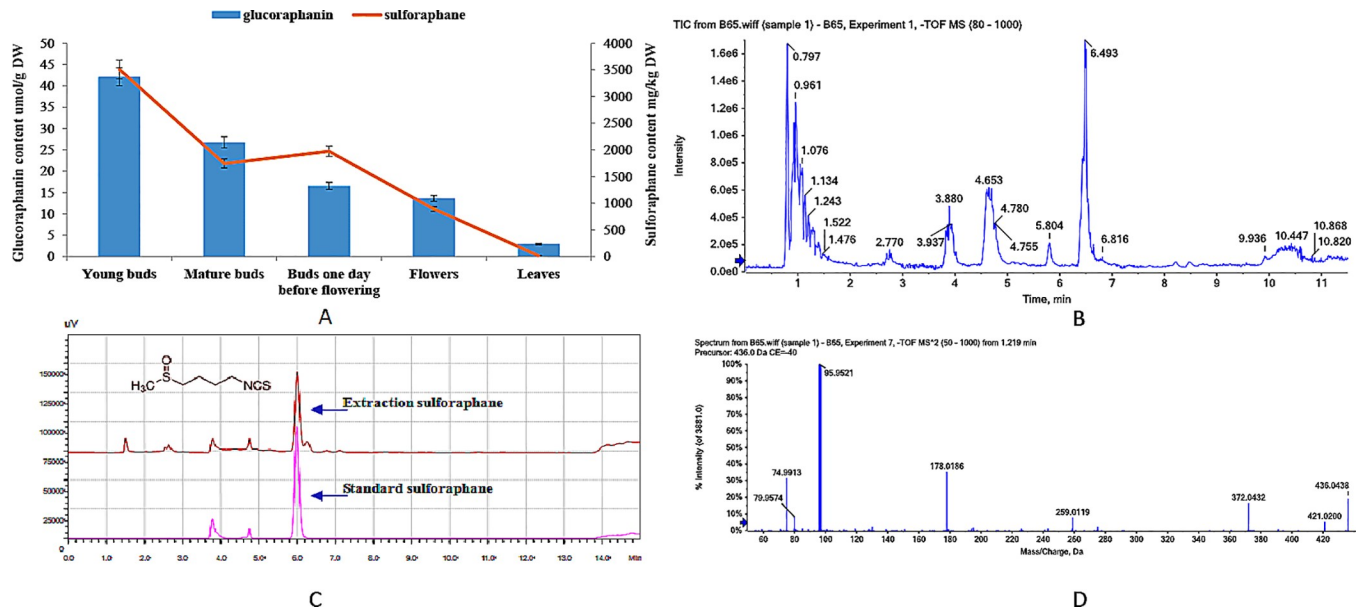


Fig 6. Sulforaphane and glucoraphanin concentrations detected in different organs of broccoli at bolting stage (A). Chromatography of sulforaphane (C) and TIC Chromatograph of glucosinolate (B) corresponding to glucoraphanin spectrum (RT) (D).

<https://doi.org/10.1371/journal.pone.0213902.g006>

increases both long- and short-chain aliphatic glucosinolates [26, 29]. In our study, *CYP79F1* (*Bo5g021810-4.2906*) was only significantly up-regulated in aliphatic glucosinolate biosynthesis, however this up-regulation was not found in the other developing buds and leaves. Therefore, up-regulation of the *CYP79F1* gene might be one of the reasons for causing sulforaphane content being higher in young buds than mature buds, blossom buds, flowers and leaves at bolting stage, and this result was also supported by qRT-PCR. So up-regulation of the *CYP79F1* gene might directly affect glucoraphanin accumulation [22, 31]. In growing and developing buds, because there is no up-regulation of the *CYP79F1* gene, so the intermediates and precursors of glucoraphanin are gradually consumed. Therefore, the results of our study support de novo synthesis of glucoraphanin in young buds. Recent studies have identified two mechanisms of glucosinolate metabolism in plants: transport and de novo synthesis. The first mechanism is the transport of glucosinolate via the phloem from mature leaves to inflorescences and fruits [66, 67]. Other studies have shown that reproductive organs are likely to generate specific and unique glucosinolates by de novo synthesis in these organs [22, 68]. In fact, divergent glucosinolate composition of seeds and other organs have been widely detected, and there are obviously different amounts in the seeds, higher than the other organs, which also supports the possibility of de novo synthesis in reproductive organs [69]. Our study provided for evidence in synthesis of glucosinolate in reproductive organs. *St5b-2* is numbered K11821 in the KEGG orthology pathway, and it is responsible for tryptophan metabolism, glucosinolate biosynthesis, biosynthesis of secondary metabolites, and 2-Oxocarboxylic acid metabolism. In our study, this gene referred to 4-methylthiobutyl-glucosinolate biosynthesis. According to sequence analysis, another gene in this family, *ST5a-1*, has similar function in tryptophan metabolism, glucosinolate biosynthesis, biosynthesis of secondary metabolites, and 2-Oxocarboxylic acid metabolism. *ST5a-1* and *St5b-2* have been reported in *B. rapa*, and their sequences have been analyzed by shotgun sequencing, but still no similar sequence was found in broccoli [35, 37]. In this result, there was a lower level of gene expression in developmental buds compared with in leaves. This might indicate that it supported the accumulation of

4-methylthiobutyl glucosinolate (glucoerucin) for glucoraphanin generated by oxidation by *FMO GS-OX1* gene [58].

The *FMO GS-OX* family (flavin-monooxygenase) contains five genes of *FMO GS-OX1*~5, two genes of *FMO GS-OX2* and *FMO GS-OX5* [70–72], and *FMOGS-OX1* has been identified as an enzyme in the biosynthesis of aliphatic glucosinolates in *Arabidopsis*, catalyzing the S-oxygenation of methylthioalkyl to methylsulfinylalkyl glucosinolate. In sulforaphane synthesis, *FMOGS-OX1* catalyzes the conversion of 4-methylthiobutyl glucosinolate (glucoerucin) to 4-methylsulfinylbutyl glucosinolate (glucoraphanin), the precursor of sulforaphane [72–73]. Five *FMO* genes At1g65860 (*FMO GS-OX1*), At1g62540 (*FMO GS-OX2*), At1g62560 (*FMO GS-OX3*), At1g62570 (*FMO GS-OX4*), and At1g12140 (*FMO GS-OX5*) have been found within a subclade of the *FMO* phylogeny [31, 57]. In the study, the gene expression of *FMO GS-OX1* was at a low level in developing buds comparing to in leaves, which was similar to the genes of *MAM1* and *St5b-2*, suggesting the similar gene expression patterns of *St5b-2* and *FMO GS-OX1*. Most of studies have reported the hydrolysis products of glucosinolate are controlled by epithiospecifier protein (ESP), myrosinase (MY), and potentially free iron and pH [21, 74]. Previous conclusions have shown that the system of glucosinolate hydrolysis is complex, and some results suggest that the ESP runs functions via interactions with myrosinase [32]. Myrosinase can catalyze the hydrolysis of the thioglucoside linkage and release a glucose and an unstable aglycone. The aglycone moiety subsequently rearranges to form various products depending on the aglycone structure, myrosinase, pH, ferrous ion, zinc and magnesium concentrations [24, 75–77]. Our results showed a high consistency of the gene expression among *MY*, *FMO GS-OX1*, *St5b-2* and *MAM1*. Therefore, the correlations of ten genes in expression level and the contents of sulforaphane and glucoraphanin were analyzed by Pearson correlation test. The result revealed that six genes of *MAM1*, *St5b-2*, *FMO GS-OX1*, *AOP2*, *ESP* and *ESM1* were highly correlated with correlation coefficients from 0.887 to 0.999 ($P < 0.01$) (Tables 6 and 7). From the contents and consistent changes of glucoraphanin and sulforaphane, it could be proved that myrosinase and ESP had not influence on sulforaphane generation at bolting stage.

So far, three *AOP2* genes have been identified in *B. oleracea*, two are non-functional due to the presence of premature stop codons, and no *AOP3* gene has been found [35]. In contrast, all three *AOP2* copies are functional in *B. rapa*, resulting in conversion of glucoraphanin into gluconapin, which explains why glucoraphanin is abundant in *B. oleracea*, but not in *B. rapa* [31, 35]. *AOP3* also does not exist in *B. rapa*, which contains three *AOP* loci orthologs, each containing two tandem duplicated genes [21, 60]. Studies in *Arabidopsis* have shown differential *AOP* leaf expression, whereby a particular accession expresses either *AOP2* or *AOP3* but not both [70, 78], which has been reported to be due a complete inversion of the *AOP2* and *AOP3* structural genes in some accessions, causing the *AOP3* gene to be expressed from the *AOP2* promoter [79]. This conclusion is in conflict with the absence of an *AOP3* gene in cabbage [35], but our results support this conclusion in *Arabidopsis* based on *AOP3* gene expression in this study.

According to the gene expression patterns of *AOP2* and *AOP3*, it was found that *AOP2* gene, likely *MY*, *FMO GS-OX1*, *St5b-2* or *MAM1*, showed a lower level of expression in developing buds than in leaves (Fig 5). However, there was significantly higher *AOP3* expression in developmental buds compared to leaves (Fig 5), the highest being in flowers, followed by young buds, mature buds and buds one day before flowering, and leaves were at the lowest level. *AOP3* should be present in broccoli plant, however it was detected in the expression of the *AOP3* domain, which might provide us new evidence for explaining the diversity of sulforaphane in different broccoli organs. Meanwhile the *AOP3* gene plays a role in hydroxylation of glucoraphanin, which might partly explain why there was lower accumulation of

Table 6. The correlation analysis of sulforaphane contents and related genes in different organs.

Pearson Correlation	Sulforaphane	MAMI	IMS2	CYP79F1	FMO GS-OX1	AOP2	AOP3	MY	St5b-2	ESP	ESM1
Sulforaphane	1	-0.61	-0.373	0.796	-0.581	-0.51	0.125	-0.468	-0.63	-0.141	0.039
MAMI	-0.61	1	0.06	-0.198	.994**	.967**	-0.484	.979**	.999**	0.868	0.757
IMS2	-0.373	0.06	1	-0.022	0.093	-0.002	0.828	-0.002	0.055	-0.124	-0.144
CYP79F1	0.796	-0.198	-0.022	1	-0.123	-0.045	0.248	-0.015	-0.224	0.282	0.464
FMOGS-OX1	-0.581	.994**	0.093	-0.123	1	.985**	-0.443	.990**	.993**	.887*	0.79
AOP2	-0.51	.967**	-0.002	-0.045	.985**	1	-0.502	.992**	.967**	.907*	0.828
AOP3	0.125	-0.484	0.828	0.248	-0.443	-0.502	1	-0.498	-0.493	-0.494	-0.426
MY	-0.468	.979**	-0.002	-0.015	.990**	.992**	-0.498	1	.975**	.939*	0.862
St5b-2	-0.63	.999**	0.055	-0.224	.993**	.967**	-0.493	.975**	1	0.855	0.74
ESP	-0.141	0.868	-0.124	0.282	.887*	.907*	-0.494	.939*	0.855	1	.980**
ESM1	0.039	0.757	-0.144	0.464	0.79	0.828	-0.426	0.862	0.74	.980**	1

Note: *. Correlation is significant at the 0.05 level (2-tailed) and

** . Correlation is significant at the 0.01 level (2-tailed).

<https://doi.org/10.1371/journal.pone.0213902.t006>

glucoraphanin in flowers compared to the other developmental buds, resulting in low concentration of sulforaphane [41, 60].

Plant hormones in pathways affecting glucoraphanin accumulation

Some studies have reported glucoraphanin and sulforaphane are influenced by genotype, developmental stages and environment effects, and others state that plant hormones, such as IAA and jasmonic acid (JA), also affect glucoraphanin production, resulting in changes in sulforaphane levels in broccoli [22–24, 57]. Several reports indicate that the loss function of CYP79F1 in mutations could end the formation of short-chain methionine-derived glucosinolates, but increase the amounts of IAA and cytokinin [80]. Glucosinolate syntheses also conversely affect the levels of auxin and cytokinin [27, 80]. JA is an elicitor and signaling molecule for glucosinolate biosynthesis, it has been shown to enhance both the production of indolic glucosinolates and their biosynthetic gene transcript levels in *Arabidopsis*, and the accumulation of glucoraphanin in broccoli could be up-regulated by JA related genes [38, 81].

Table 7. The correlation analysis of glucoraphanin contents and related genes in different organs.

Pearson Correlation	glucoraphanin	MAMI	IMS2	CYP79F1	FMO GS-OX1	AOP2	AOP3	MY	St5b-2	ESP	ESM1
glucoraphanin	1	-.634	-.444	.768	-.587	-.473	.061	-.470	-.647	-.183	.000
MAMI	-.634	1	.060	-.198	.994**	.967**	-.484	.979**	.999**	.868	.757
IMS2	-.444	.060	1	-.022	.093	-.002	.828	-.002	.055	-.124	-.144
CYP79F1	.768	-.198	-.022	1	-.123	-.045	.248	-.015	-.224	.282	.464
FMOGS-OX1	-.587	.994**	.093	-.123	1	.985**	-.443	.990**	.993**	.887*	.790
AOP2	-.473	.967**	-0.002	-0.045	.985**	1	-.502	.992**	.967**	.907*	.828
AOP3	.061	-.484	.828	.248	-.443	-.502	1	-.498	-.493	-.494	-.426
MY	-.470	.979**	-0.002	-0.015	.990**	.992**	-.498	1	.975**	.939*	.862
St5b-2	-.647	.999**	.055	-.224	.993**	.967**	-.493	.975**	1	.855	.740
ESP	-.183	.868	-.124	.282	.887*	.907*	-.494	.939*	.855	1	.980**
ESM1	.000	.757	-.144	.464	.790	.828	-.426	.862	.740	.980**	1

Note: *. Correlation is significant at the 0.05 level (2-tailed) and

** . Correlation is significant at the 0.01 level (2-tailed).

<https://doi.org/10.1371/journal.pone.0213902.t007>

In this study, plant hormone signal transduction was analyzed by RNA sequencing, and there were 95, 89, 97 and 86 corresponding DEGs with the same 521 background genes based on the developing buds (LN_B1- 4) versus leaf expression. According to the differences in plant hormone signal transduction gene expression among four organs in developmental buds, 2 DEGs were found in the auxin signaling pathway, one was up-regulated (*Bo5g027930*) only in young buds. This finding reminded us the association of young buds with higher sulforaphane content and higher expression of *Bo5g027930* only occurring in this organ, which might provide evidence for the importance of *CYP79F1*. The specific mechanism driving these observations still needs further research. The other auxin signaling gene was down regulated (*Bo9g151530*), and it occurred in buds one day before flowering and flowers. Thus, it could be inferred that different auxin response might affect the accumulation of glucoraphanin [27, 41].

In the cytokinin signaling pathway, 3 up-regulated genes and 2 down-regulated genes were different in developing buds. A total of 3 up-regulated genes, *Bo8g091410*, *Bo3g107060* and *Bo3g035110*, only showed higher expression in young buds and were absent in the remaining developing buds. In contrast, 2 genes, *Bo5g027070* and *Bo8g059410*, were down-regulated in buds one day before flowering and flowers, and absent from in young and mature buds. These 5 genes belong to the two-component response regulator ARR-A family, which might be potential genes in affecting glucoraphanin generation [29].

Conclusions

In the study, it was found that *CYP79F1* plays a fundamental and direct role in sulforaphane production of inflorescences at differential developmental stages, and a low expression level resulted in a decrease of this compound or the precursor glucoraphanin due to competition for the intermediates, such as 2-oxo-6-methylthihexanoic acid or 4-methylthiobutyl (glucoerucin). These genes of *MAM1*, *MAM3*, *St5b-2*, *FMO GS-OX1* were in favor of glucoraphanin, *MY*, *ESP* and *ESM1* played a high efficiency function in sulforaphane generation although with low expression level in this stage. At the same time, the plant hormones auxin and cytokinin might affect glucoraphanin accumulation. The knowledge gained from this study provides a way to study different molecular mechanisms and the diversity of sulforaphane in different organs during broccoli development stages.

Supporting information

S1 Fig. The most enriched GO terms.

(TIF)

S2 Fig. Patterns of gene expressions in the developmental buds and leaves of B52 by STEM analysis ($P < 0.05$). The green line represents the expression pattern of all the genes. The number of genes belonging to each pattern is labeled above frame.

(TIF)

S3 Fig. The distribution of clean reads, containing N, low quality and adapter related reads in the raw reads.

(TIF)

Acknowledgments

This work was funded by the National Key Research and Development Program of China (2017YFD0101805), the National Nature Science Foundation (31501761, 31372067), the China Agriculture Research System (CARS-23-A8), as well as the Science and Technology

Innovation Program of the Chinese Academy of Agricultural Sciences (CAAS-ASTIP-IVFCAAS).

Author Contributions

Conceptualization: Zhansheng Li.

Data curation: Zhansheng Li, Yumei Liu, Honghao Lv.

Formal analysis: Zhansheng Li, Yumei Liu.

Funding acquisition: Zhansheng Li, Yumei Liu.

Investigation: Zhansheng Li, Limei Yang, Mu Zhuang.

Methodology: Zhansheng Li, Lingyun Li, Yangyong Zhang.

Project administration: Zhansheng Li.

Resources: Zhansheng Li.

Software: Zhansheng Li.

Supervision: Zhiyuan Fang.

Validation: Zhansheng Li.

Writing – original draft: Zhansheng Li.

Writing – review & editing: Zhansheng Li.

References

1. Jin CY, Moon DO, Lee JD, Heo MS, Choi YH, Lee CM, et al. Sulforaphane sensitizes tumor necrosis factor-related apoptosis-inducing ligand-mediated apoptosis through downregulation of ERK and Akt in lung adenocarcinoma A549 cells. *Carcinogenesis* 2007; 28(5): 1058–66. <https://doi.org/10.1093/carcin/bgl251> PMID: 17183064
2. Chung YK, Chi-Hung OR, Lu CH, Ouyang WT, Yang SY, Chang CC. Sulforaphane down-regulates SKP2 to stabilize p27 for inducing antiproliferation in human colon adenocarcinoma cells. *J Biosci Bioeng* 2015; 119(1): 35–42. <https://doi.org/10.1016/j.jbiosc.2014.06.009> PMID: 25070589
3. Kallifatidis G, Rausch V, Baumann B, Apel A, Beckermann BM, Groth A, et al. Sulforaphane targets pancreatic tumour-initiating cells by NF-kappa B-induced antiapoptotic signalling. *Gut* 2009; 58(7): 949–963. <https://doi.org/10.1136/gut.2008.149039> PMID: 18829980
4. Azarenko O, Okouneva T, Singletary KW, Jordan MA, and Wilson L. Suppression of microtubule dynamic instability and turnover in MCF7 breast cancer cells by sulforaphane. *Carcinogenesis* 2008; 29(12): 2360–8. <https://doi.org/10.1093/carcin/bgn241> PMID: 18952594
5. Abbaoui B, Riedl KM, Ralston RA, Thomas-Ahner JM, Schwartz SJ, Clinton SK, et al. Inhibition of bladder cancer by broccoli isothiocyanates sulforaphane and erucin: characterization, metabolism, and interconversion. *Mol Nutr Food Res* 2012; 56(11): 1675–1687. <https://doi.org/10.1002/mnfr.201200276> PMID: 23038615
6. Brooks JD, Paton V. Potent induction of carcinogen defence enzymes with sulforaphane, a putative prostate cancer chemopreventive agent. *Prostate Cancer Prostatic Dis* 1999; 2(S3): S8. <https://doi.org/10.1038/sj.pcan.4500334> PMID: 12496788
7. Zhang R, Miao QW, Zhu CX, Zhao Y, Liu L, Yang J, et al. Sulforaphane Ameliorates Neurobehavioral Deficits and Protects the Brain From Amyloid beta Deposits and Peroxidation in Mice With Alzheimer-Like Lesions. *Am J Alzheimers Dis Other Dement* 2014. 30(2): 183–191. <https://doi.org/10.1177/1533317514542645> PMID: 25024455
8. Evans PC. The influence of sulforaphane on vascular health and its relevance to nutritional approaches to prevent cardiovascular disease. *EPMA J* 2011; 2(1): 9–14. <https://doi.org/10.1007/s13167-011-0064-3> PMID: 23199123
9. Sivakumar MR, Sanjeev S. Cerebrovascular manifestations and carotid artery intima medial thickness in Takayasu's arteritis evaluated by using the Disease Extent Index for TA (DEI.Tak). *Clinical and Experimental Rheumatology* 2007; 25(2): S120–S120.

10. Alumkal JJ, Slottke R, Schwartzman J, Cherala G, Munar M, Graff JN, et al. A phase II study of sulforaphane-rich broccoli sprout extracts in men with recurrent prostate cancer. *Investigational New Drugs* 2015; 33(2): 480–489. <https://doi.org/10.1007/s10637-014-0189-z> PMID: 25431127
11. Angeloni C, Leoncini E, Malaguti M, Angelini S, Hrelia P, Hrelia S. Modulation of phase II enzymes by sulforaphane: implications for its cardioprotective potential. *J Agric Food Chem* 2009; 57(12): 5615–22. <https://doi.org/10.1021/jf900549c> PMID: 19456137
12. Asakage M, Tsuno NH, Kitayama J, Tsuchiya T, Yoneyama S, Yamada J, et al. Sulforaphane induces inhibition of human umbilical vein endothelial cells proliferation by apoptosis. *Angiogenesis* 2006; 9(2): 83–91. <https://doi.org/10.1007/s10456-006-9034-0> PMID: 16821112
13. Ferreira de Oliveira JM, Remedios C, Oliveira H, Pinto P, Pinho F, Pinho S, et al. Sulforaphane induces DNA damage and mitotic abnormalities in human osteosarcoma MG-63 cells: correlation with cell cycle arrest and apoptosis. *Nutr Cancer* 2014; 66(2): 325–34. <https://doi.org/10.1080/01635581.2014.864777> PMID: 24405297
14. Angelino D, Dosz EB, Sun J, Hoeflinger JL, Van Tassel ML, Chen P, et al. Myrosinase-dependent and -independent formation and control of isothiocyanate products of glucosinolate hydrolysis. *Frontiers in Plant Science* 2015; 6: 831. <https://doi.org/10.3389/fpls.2015.00831> PMID: 26500669
15. Fahey JW, Holtzclaw WD, Wehage SL, Wade KL, Stephenson KK, Talalay P. Sulforaphane Bioavailability from Glucoraphanin-Rich Broccoli: Control by Active Endogenous Myrosinase. *Plos One* 2015; 10(11): e0140963. <https://doi.org/10.1371/journal.pone.0140963> PMID: 26524341
16. Angelino D, Jeffery E. Glucosinolate hydrolysis and bioavailability of resulting isothiocyanates: Focus on glucoraphanin. *Journal of Functional Foods* 2014; 7: 67–76.
17. Cramer JM, Jeffery EH. A comparison of the bioavailability of sulforaphane from broccoli sprouts and a semi-purified broccoli powder rich in glucoraphanin in healthy human males. *Faseb Journal* 2009; 23.
18. Matusheski NV, Jeffery EH. Comparison of the bioactivity of two glucoraphanin hydrolysis products found in broccoli, sulforaphane and sulforaphane nitrile. *J Agric Food Chem* 2001; 49(12): 5743–9. PMID: 11743757
19. Agudo A, Ibanez R, Amiano P, Ardanaz E, Barricarte A, Berenguer A, et al. Consumption of cruciferous vegetables and glucosinolates in a Spanish adult population. *European Journal of Clinical Nutrition* 2008; 62(3): 324–331. <https://doi.org/10.1038/sj.ejcn.1602750> PMID: 17426741
20. Ares AM, Bernal J, Nozal MJ, Turner C, Plaza M. Fast determination of intact glucosinolates in broccoli leaf by pressurized liquid extraction and ultra-high performance liquid chromatography coupled to quadrupole time-of-flight mass spectrometry. *Food Research International* 2015; 76(Pt 3): 498–505. <https://doi.org/10.1016/j.foodres.2015.06.037> PMID: 28455030
21. Brown PD, Tokuhisa JG, Reichelt M, Gershenzon J. Variation of glucosinolate accumulation among different organs and developmental stages of *Arabidopsis thaliana*. *Phytochemistry* 2003; 62(3): 471–81. PMID: 12620360
22. Field B, Cardon G, Traka M, Botterman J, Vancanneyt G, Mithen R. Glucosinolate and amino acid biosynthesis in *Arabidopsis*. *Plant Physiology* 2004; 135: 828–839. <https://doi.org/10.1104/pp.104.039347> PMID: 15155874
23. Grubb CD, Abel S. Glucosinolate metabolism and its control. *Trends in Plant Science* 2006; 11(2): 89–100. <https://doi.org/10.1016/j.tplants.2005.12.006> PMID: 16406306
24. Halkier BA, Gershenzon J. Biology and biochemistry of glucosinolates. *Annual Review of Plant Biology* 2006; 57(1): 303–333.
25. Brader G, Mikkelsen MD, Halkier BA, Palva ET. Altering glucosinolate profiles modulates disease resistance in plants. *Plant Journal* 2006; 46(5): 758–767. <https://doi.org/10.1111/j.1365-313X.2006.02743.x> PMID: 16709192
26. Chen SX, Glawischnig E, Jorgensen K, Naur P, Jorgensen B, Olsen CE, et al. CYP79F1 and CYP79F2 have distinct functions in the biosynthesis of aliphatic glucosinolates in *Arabidopsis*. *Plant Journal* 2003; 33(5): 923–937. PMID: 12609033
27. Wittstock U, Halkier BA. Glucosinolate research in the *Arabidopsis* era. *Trends in Plant Science* 2002; 7(6): 263–270. PMID: 12049923
28. Guo LP, Yang RQ, Wang ZY, Guo QH, Gu ZX. Glucoraphanin, sulforaphane and myrosinase activity in germinating broccoli sprouts as affected by growth temperature and plant organs. *Journal of Functional Foods* 2014; 9(1): 70–77.
29. Sonderby IE, Geu-Flores F, Halkier BA. Biosynthesis of glucosinolates—gene discovery and beyond. *Trends in Plant Science* 2010; 15(5): 283–290. <https://doi.org/10.1016/j.tplants.2010.02.005> PMID: 20303821

30. Hansen CH, Du LC, Naur P, Olsen CE, Axelsen KB, Hick AJ, et al. CYP83B1 is the oxime-metabolizing enzyme in the glucosinolate pathway in Arabidopsis. *Journal of Biological Chemistry* 2001; 276(6): 24790–24796.
31. Kliebenstein DJ, Kroymann J, Brown P, Figuth A, Pedersen D, Gershenzon J, et al. Genetic control of natural variation in Arabidopsis glucosinolate accumulation. *Plant Physiol* 2001; 126(2): 811–25. PMID: [11402209](https://pubmed.ncbi.nlm.nih.gov/11402209/)
32. Lambrix V, Reichelt M, Mitchell-Olds T, Kliebenstein DJ, Gershenzon J. The Arabidopsis epithiospecifier protein promotes the hydrolysis of glucosinolates to nitriles and influences *Trichoplusia ni* herbivory. *Plant Cell* 2001; 13(12): 2793–2807. <https://doi.org/10.1105/tpc.010261> PMID: [11752388](https://pubmed.ncbi.nlm.nih.gov/11752388/)
33. Fahey JW, Zalcmann AT, Talalay P. The chemical diversity and distribution of glucosinolates and isothiocyanates among plants. *Phytochemistry* 2001; 56(1): 5–51. PMID: [11198818](https://pubmed.ncbi.nlm.nih.gov/11198818/)
34. Kensler TW, Ng D, Carmella SG, Chen M, Jacobson LP, Munoz A, et al. Modulation of the metabolism of airborne pollutants by glucoraphanin-rich and sulforaphane-rich broccoli sprout beverages in Qidong, China. *Carcinogenesis* 2012; 33(1): 101–7. <https://doi.org/10.1093/carcin/bgr229> PMID: [22045030](https://pubmed.ncbi.nlm.nih.gov/22045030/)
35. Liu SY, Liu YM, Yang XH, Tong CB, Edwards D, Parkin IAP, et al. The Brassica oleracea genome reveals the asymmetrical evolution of polyploid genomes. *Nature Communications* 2014; 5: 3930. <https://doi.org/10.1038/ncomms4930> PMID: [24852848](https://pubmed.ncbi.nlm.nih.gov/24852848/)
36. Cheng F, Mandakova T, Wu J, Xie Q, Lysak MA, et al. Deciphering the Diploid Ancestral Genome of the Mesoheptaploid *Brassica rapa*. *Plant Cell* 2013; 25(5): 1541–1554. <https://doi.org/10.1105/tpc.113.110486> PMID: [23653472](https://pubmed.ncbi.nlm.nih.gov/23653472/)
37. Wang XW, Wang HZ, Wang J, Sun RF, Wu J, Liu SY, et al. The genome of the mesopolyploid crop species *Brassica rapa*. *Nature Genetics* 2011; 43(10): 1035–9. <https://doi.org/10.1038/ng.919> PMID: [21873998](https://pubmed.ncbi.nlm.nih.gov/21873998/)
38. Guo LP, Yang RQ, Gu ZX. Cloning of genes related to aliphatic glucosinolate metabolism and the mechanism of sulforaphane accumulation in broccoli sprouts under jasmonic acid treatment. *Journal of the Science of Food and Agriculture* 2016; 96(13): 4329–4336. <https://doi.org/10.1002/jsfa.7629> PMID: [26786856](https://pubmed.ncbi.nlm.nih.gov/26786856/)
39. Hansen BG, Kliebenstein DJ, Halkier BA. Identification of a flavin-monooxygenase as the S-oxygenating enzyme in aliphatic glucosinolate biosynthesis in Arabidopsis. *Plant Journal* 2007; 50(5): 902–910. <https://doi.org/10.1111/j.1365-3113.2007.03101.x> PMID: [17461789](https://pubmed.ncbi.nlm.nih.gov/17461789/)
40. Li YM, Sawada Y, Hirai A, Sato M, Kuwahara A, Yan XF, et al. Altered Regulation of MYB Genes Changes the Aliphatic Glucosinolate Accumulation Under Long-Term Sulfur Deficiency in Arabidopsis. *Molecular Physiology and Ecophysiology of Sulfur* 2015; 195–199.
41. Li ZS, Liu YM, Fang ZY, Yang LM, Zhuang M, Zhang YY, et al. Variation of Sulforaphane Levels in Broccoli (*Brassica Oleracea* Var. *Italica*) during Flower Development and the Role of Gene Aop2. *Journal of Liquid Chromatography & Related Technologies* 2014; 37(9): 1199–1211.
42. Glade MJ, Meguid MM. A Glance at . . . Broccoli, glucoraphanin, and sulforaphane. *Nutrition* 2015; 31(9): 1175–1178. <https://doi.org/10.1016/j.nut.2015.03.003> PMID: [26004191](https://pubmed.ncbi.nlm.nih.gov/26004191/)
43. Iori R, Bernardi R, Gueyrard D, Rollin P, Palmieri S. Formation of glucoraphanin by chemoselective oxidation of natural glucoerucin: a chemoenzymatic route to sulforaphane. *Bioorg Med Chem Lett* 1999; 9(7): 1047–8. PMID: [10230637](https://pubmed.ncbi.nlm.nih.gov/10230637/)
44. Cano-Gomez C, Palero F, Buitrago MD, Garcia-Casado MA, Fernandez-Pinero J, Fernandez-Pacheco P, et al. Analyzing the genetic diversity of teschoviruses in Spanish pig populations using complete VP1 sequences. *Infection Genetics and Evolution* 2011; 11(8): 2144–2150.
45. Heini S, Spath K, Egger E, Grabherr R. Sequence analysis and characterization of two cryptic plasmids derived from *Lactobacillus buchneri* CD034. *Plasmid* 2011; 66(3): 159–168. <https://doi.org/10.1016/j.plasmid.2011.08.002> PMID: [21907734](https://pubmed.ncbi.nlm.nih.gov/21907734/)
46. Clark CG, Beeston A, Bryden L, Wang GH, Barton C, Cuff W, et al. Phylogenetic relationships of *Campylobacter jejuni* based on porA sequences. *Canadian Journal of Microbiology* 2007; 53(1): 27–38. <https://doi.org/10.1139/w06-099> PMID: [17496947](https://pubmed.ncbi.nlm.nih.gov/17496947/)
47. Nolling J, Breton G, Omelchenko MV, Makarova KS, Zeng QD, Gibson R, et al. Genome sequence and comparative analysis of the solvent-producing bacterium *Clostridium acetobutylicum*. *Journal of Bacteriology* 2001; 183(16): 4823–4838. <https://doi.org/10.1128/JB.183.16.4823-4838.2001> PMID: [11466286](https://pubmed.ncbi.nlm.nih.gov/11466286/)
48. Clark RM, Schweikert G, Toomajian C, Ossowski S, Zeller G, Shinn P, et al. Common sequence polymorphisms shaping genetic diversity in Arabidopsis thaliana. *Science* 2007; 317(5836): 338–342. <https://doi.org/10.1126/science.1138632> PMID: [17641193](https://pubmed.ncbi.nlm.nih.gov/17641193/)
49. Li B, Dewey CN. RSEM: accurate transcript quantification from RNA-Seq data with or without a reference genome. *Bmc Bioinformatics* 2011; 12(1): 323.

50. Zhang XL, Liu YM, Fang ZY, Li ZS, Yang LM, Zhuang M, et al. Comparative Transcriptome Analysis between Broccoli (*Brassica oleracea* var. *italica*) and Wild Cabbage (*Brassica macrocarpa* Guss.) in Response to Plasmiodiophorabraceae during Different Infection Stages. *Frontiers in Plant Science* 2016; 7(R106): 1929.
51. Liu C, Liu ZY, Li CY, Zhang Y, Feng H. Comparative transcriptome analysis of fertile and sterile buds from a genetically male sterile line of Chinese cabbage. *In Vitro Cellular & Developmental Biology-Plant* 2016; 52(2): 130–139.
52. Xing MM, Lv HH, Ma J, Xu DH, Li HL, Yang LM, et al. Transcriptome Profiling of Resistance to *Fusarium oxysporum* f. sp. *conglutinans* in Cabbage (*Brassica oleracea*) Roots. *Plos One* 2016; 11(2): e0148048. <https://doi.org/10.1371/journal.pone.0148048> PMID: 26849436
53. Li ZS, Liu YM, Fang ZY, Yang LM, Zhuang M, Zhang YY, et al. Development and Identification of Anti-cancer Component of Sulforaphane in Developmental Stages of Broccoli (*Brassica oleracea* var. *italica*). *Journal of Food and Nutrition Research* 2016; 4(8): 490–497.
54. Agerbirk N, Olsen CE, Chew FS, Orgaard M. Variable glucosinolate profiles of *Cardamine pratensis* (*Brassicaceae*) with equal chromosome numbers. *J Agric Food Chem* 2010; 58(8): 4693–4700. <https://doi.org/10.1021/jf904362m> PMID: 20334382
55. Gao MQ, Li GY, Yang B, McCombie WR, Quiros CF. Comparative analysis of a Brassica BAC clone containing several major aliphatic glucosinolate genes with its corresponding Arabidopsis sequence. *Genome* 2004; 47(4): 666–679. <https://doi.org/10.1139/g04-021> PMID: 15284871
56. Giamoustaris A, Mithen R. The effect of flower colour and glucosinolates on the interaction between oil-seed rape and pollen beetles. *Entomologia Experimentalis Et Applicata* 1996; 80(1): 206–208.
57. Halkier BA, Du LC. The biosynthesis of glucosinolates. *Trends in Plant Science* 1997; 2(11): 425–431.
58. Hall C, McCallum D, Prescott A, Mithen R. Biochemical genetics of glucosinolate modification in Arabidopsis and Brassica. *Theoretical and Applied Genetics* 2001; 102(2): 369–374.
59. Hansen BG, Kerwin RE, Ober JA, Lambrix VM, Mitchell-Olds T, Gershenzon J, et al. A Novel 2-Oxoacid-Dependent Dioxygenase Involved in the Formation of the Goiterogenic 2-Hydroxybut-3-enyl Glucosinolate and Generalist Insect Resistance in Arabidopsis. *Plant Physiology* 2008; 148(4): 2096–2108. <https://doi.org/10.1104/pp.108.129981> PMID: 18945935
60. Li G, Quiros CF. In planta side-chain glucosinolate modification in Arabidopsis by introduction of dioxygenase Brassica homolog BoGSL-ALK. *Theoretical and Applied Genetics* 2003; 106(6): 1116–1121. <https://doi.org/10.1007/s00122-002-1161-4> PMID: 12671761
61. Burow M, Atwell S, Francisco M, Kerwin RE, Halkier BA, Kliebenstein DJ. The Glucosinolate Biosynthetic Gene AOP2 Mediates Feed-back Regulation of Jasmonic Acid Signaling in Arabidopsis. *Molecular Plant* 2015; 8(8): 1201–1212. <https://doi.org/10.1016/j.molp.2015.03.001> PMID: 25758208
62. Heidel AJ, Clauss MJ, Kroymann J, Savolainen O, Mitchell-Olds T. Natural variation in MAM within and between populations of Arabidopsis lyrata determines glucosinolate phenotype. *Genetics* 2006; 173(3): 1629–36. <https://doi.org/10.1534/genetics.106.056986> PMID: 16702431
63. Piotrowski M, Schemenewitz A, Lopukhina A, Muller A, Janowitz T, Weiler EW, et al. Desulfoglucosinolate sulfotransferases from Arabidopsis thaliana catalyze the final step in the biosynthesis of the glucosinolate core structure. *Journal of Biological Chemistry* 2004; 279(49): 50717–50725. <https://doi.org/10.1074/jbc.M407681200> PMID: 15358770
64. Yabar E, Pedreschi R, Chirinos R, Campos D. Glucosinolate content and myrosinase activity evolution in three maca (*Lepidium meyenii* Walp.) ecotypes during preharvest, harvest and postharvest drying. *Food Chemistry* 2011; 127(4): 1576–1583.
65. Textor S, de Kraker JW, Hause B, Gershenzon J, Tokuhisa JG. MAM3 catalyzes the formation of all aliphatic glucosinolate chain lengths in Arabidopsis. *Plant Physiology* 2007; 144(1): 60–71. <https://doi.org/10.1104/pp.106.091579> PMID: 17369439
66. Brudenell AJP, Griffiths H, Rossiter JT, Baker DA. The phloem mobility of glucosinolates. *Journal of Experimental Botany* 1999; 50(335): 745–756.
67. Chen S, Andreasson E. Update on glucosinolate metabolism and transport. *Plant Physiology and Biochemistry* 2001; 39(9): 743–758.
68. Du LC, Halkier BA. Biosynthesis of glucosinolates in the developing silique walls and seeds of *Sinapis alba*. *Phytochemistry* 1998; 48(7): 1145–1150.
69. Gorissen A, Kraut NU, de Visser R, de Vries M, Roelofsen H, Vonk RJ. No de novo sulforaphane biosynthesis in broccoli seedlings. *Food Chemistry* 2011; 127(1): 192–196.
70. Bennett RN, Hick AJ, Dawson GW, Wallsgrove RM. Glucosinolate Biosynthesis—Further Characterization of the Aldoxime Forming Microsomal Monooxygenases in Oilseed Rape Leaves. *Plant Physiology* 1995; 109(1): 299–305. PMID: 12228596

71. Kong WW, Li J, Yu QY, Cang W, Xu R, Wang Y, et al. Two Novel Flavin-Containing Monooxygenases Involved in Biosynthesis of Aliphatic Glucosinolates. *Frontiers in Plant Science* 2016; 7(e2068):1292.
72. Li J, Hansen BG, Ober JA, Kliebenstein DJ, Halkier BA. Subclade of Flavin-Monooxygenases Involved in Aliphatic Glucosinolate Biosynthesis. *Plant Physiology* 2008; 148(3): 1721–1733. <https://doi.org/10.1104/pp.108.125757> PMID: 18799661
73. Li J, Kristiansen KA, Hansen BG, Halkier BA. Cellular and subcellular localization of flavin-monooxygenases involved in glucosinolate biosynthesis. *Journal of Experimental Botany* 2011; 62(3): 1337–1346. <https://doi.org/10.1093/jxb/erq369> PMID: 21078824
74. Wittstock U, Kliebenstein DJ, Lambrix V, Reichelt M, Gershenzon J. Glucosinolate hydrolysis and its impact on generalist and specialist insect herbivores. *Integrative Phytochemistry: From Ethnobotany to Molecular Ecology* 2003; 37: 101–126.
75. Liang H, Yuan QP, Xiao Q. Effects of metal ions on myrosinase activity and the formation of sulforaphane in broccoli seed. *Journal of Molecular Catalysis B-Enzymatic* 2006; 43(1): 19–22.
76. Fu LL, Wang M, Han BY, Tan DG, Sun XP, Zhang JM. Arabidopsis Myrosinase Genes AtTGG4 and AtTGG5 Are Root-Tip Specific and Contribute to Auxin Biosynthesis and Root-Growth Regulation. *International Journal of Molecular Sciences* 2016; 17(6): 892.
77. Pang QY, Guo J, Chen SX, Chen YZ, Zhang L, Fei MH, et al. Effect of salt treatment on the glucosinolate-myrosinase system in *Thellungiella salsuginea*. *Plant and Soil* 2012; 355(1–2): 363–374.
78. Kliebenstein DJ, Lambrix VM, Reichelt M, Gershenzon J, Mitchell-Olds T. Gene duplication in the diversification of secondary metabolism: Tandem 2-oxoglutarate-dependent dioxygenases control glucosinolate biosynthesis in arabidopsis. *Plant Cell* 2001; 13(3): 681–693. PMID: 11251105
79. Kroymann J, Textor S, Tokuhisa JG, Falk KL, Bartram S, Gershenzon J, et al. A gene controlling variation in arabidopsis glucosinolate composition is part of the methionine chain elongation pathway. *Plant Physiology* 2001; 127(3): 1077–1088. PMID: 11706188
80. Tantikanjana T, Mikkelsen MD, Hussain M, Halkier BA, Sundaresan V. Functional analysis of the tandem-duplicated P450 genes SPS/BUS/CYP79F1 and CYP79F2 in glucosinolate biosynthesis and plant development by Ds transposition-generated double mutants. *Plant Physiology* 2004; 135(2): 840–848. <https://doi.org/10.1104/pp.104.040113> PMID: 15194821
81. Bak S, Feyereisen R. The involvement of two P450 enzymes, CYP83B1 and CYP83A1, in auxin homeostasis and glucosinolate biosynthesis. *Plant Physiology* 2001; 127(1): 108–118. PMID: 11553739